



Holographic Van der Waals-like phase transition in the Gauss–Bonnet gravity

Song He^{c,a}, Li-Fang Li^d, Xiao-Xiong Zeng^{a,b,*}

^a State Key Laboratory of Theoretical Physics, Institute of Theoretical Physics, Chinese Academy of Sciences, Beijing 100190, China

^b School of Material Science and Engineering, Chongqing Jiaotong University, Chongqing 400074, China

^c Max Planck Institute for Gravitational Physics (Albert Einstein Institute), Am Mühlenberg 1, 14476 Golm, Germany

^d Center for Space Science and Applied Research, Chinese Academy of Sciences, Beijing 100190, China

Received 17 August 2016; received in revised form 5 December 2016; accepted 7 December 2016

Available online 12 December 2016

Editor: Stephan Stieberger

Abstract

The Van der Waals-like phase transition is observed in temperature–thermal entropy plane in spherically symmetric charged Gauss–Bonnet–AdS black hole background. In terms of AdS/CFT, the non-local observables such as holographic entanglement entropy, Wilson loop, and two point correlation function of very heavy operators in the field theory dual to spherically symmetric charged Gauss–Bonnet–AdS black hole have been investigated. All of them exhibit the Van der Waals-like phase transition for a fixed charge parameter or Gauss–Bonnet parameter in such gravity background. Further, with choosing various values of charge or Gauss–Bonnet parameter, the equal area law and the critical exponent of the heat capacity are found to be consistent with phase structures in temperature–thermal entropy plane.

© 2016 The Authors. Published by Elsevier B.V. This is an open access article under the CC BY license (<http://creativecommons.org/licenses/by/4.0/>). Funded by SCOAP³.

1. Introduction

The Van der Waals-like behavior of a black hole is an interesting phenomenon in black hole physics. It helps us to understand new phase structure in black hole thermodynamics. In the

* Corresponding author.

E-mail addresses: hesong17@gmail.com (S. He), lilf@itp.ac.cn (L.-F. Li), xxzeng@itp.ac.cn (X.-X. Zeng).

pioneering work [1], it was found that a charged AdS black hole exhibits the Van der Waals-like phase transition in the $T - S$ plane. As the charge of the black hole increases from small to large, the black hole will undergo first order phase transition and second order phase transition successively before it reaches to a stable phase, which is analogous to the van der Waals liquid–gas phase transition. The Van der Waals-like phase transition has also been observed in the $Q - \Phi$ plane [2], where Q is electric charge and Φ is the chemical potential. Further, the Van der Waals-like phase transition can be realized in the $P - V$ plane [3–10], where the negative cosmological constant is treated as the pressure P and the thermodynamical volume V is the conjugating quantity of pressure.

By AdS/CFT, [11–14] has investigated holographic entanglement entropy [15,16] in a finite volume quantum system which is dual to a spherical and charged AdS_4 black hole. Their results showed that there exists Van der Waals-like phase transition in the entanglement entropy–temperature plane. This phase transition is analogous with thermal dynamical phase transition. The critical exponent of the heat capacity for the second order phase transition was found to be consistent with that in the mean field theory. Meanwhile [17] investigated exclusively the equal area law in the entanglement entropy–temperature plane and found that the equal area law holds regardless of the size of the entangling region. There have been some extensive studies [18–23] and all the results showed that as the case of thermal dynamical entropy, the entanglement entropy exhibited the Van der Waals-like phase transition. These results indicate that there is some intrinsic relation between black hole entropy and holographic entanglement entropy. Furthermore, expectation value of Wilson loop [24–28] and the equal time two point correlation function of heavy operators have some similar properties as the entanglement entropy [29–38] to reveal the phase transitions in quantum systems.

In this paper, we would like to extend ideas in [14] to study van der Waals-like phase transitions in a Gauss–Bonnet–AdS black hole with a spherical horizon in (4+1)-dimensions in the framework of holography. Firstly, we observe that the thermal dynamical entropy will undergo the Van der Waals-like phase transition in temperature–thermal entropy plane. We also study Maxwell’s equal area law and critical exponent of the heat capacity, which are two characteristic quantities in van der Waals-like phase transition. Secondly, we would like to study the holographic entanglement entropy for a fixed size of entangled region to confirm whether there is Van der Waals-like phase transition. More precisely speaking, considering that the holographic entanglement entropy formula should have quantum correction when the bulk theory has higher curvature terms. In terms of [39–46], one can study the holographic entanglement entropy with higher derivative gravity and see what will happen for the entanglement entropy. Further, we study the expectation value of Wilson loop and two point correlation function of heavy operator in the dual field theory to check whether these two objects also undergo the Van der Waals-like phase transition. We also check the analogous equal area law and critical exponent of the analogous heat capacity, which are to make sure that all these nonlocal quantum observables will undergo van der Waals-like phase transition in the field theory dual to spherical Gauss–Bonnet–AdS black holes. Our results confirm the fact that the nonlocal quantum objects are good quantities to probe the phase structures of the spherical Gauss–Bonnet–AdS black holes.

Our paper is organized as follows. In section 2, we review the black hole thermodynamics for the spherically symmetric Gauss–Bonnet–AdS black hole and discuss the Van der Waals-like phase transition in the $T - S$ plane. We also check Maxwell’s equal area law and critical exponent of the heat capacity numerically. In section 3, with the holographic entanglement entropy, Wilson loop, and two point correlation function, we will show all these quantum objects undergo

Van der Waals-like phase transition in the spherical Gauss–Bonnet–AdS black hole. In each subsection, the equal area law is checked and the critical exponent of the analogues heat capacity is obtained via data fitting. In the final section, we present our conclusions.

Note added: While this paper was close to completion, we have found that [47] also investigate holographic phase transition for a neutral Gauss–Bonnet–AdS black hole in the extended phase space, which partially overlaps with our work.

2. Thermodynamic phase transition in the Gauss–Bonnet gravity

2.1. Review of the Gauss–Bonnet–AdS black hole

The 5-dimensional Lovelock gravity can be realized by adding the Gauss–Bonnet term to pure Einstein gravity theory. As a matter field is considered, the theory can be described by the following action [48]

$$I = \frac{1}{2\ell_p^3} \int d^5x \sqrt{-g} \left[R + \frac{12}{L^2} + \frac{\alpha L^2}{2} L_4 - 4\pi F_{\mu\nu}^{\mu\nu} \right], \tag{1}$$

with

$$L_4 = R_{\mu\nu\rho\sigma} R^{\mu\nu\rho\sigma} - 4R_{\mu\nu} R^{\mu\nu} + R^2, \tag{2}$$

where ℓ_p is Newton constant, α denotes the coupling of Gauss–Bonnet gravity, L stands for the Radius of AdS background, which satisfies the relation $L^2 = -\frac{6}{\Lambda}$, $F_{\mu\nu} = \partial_\mu A_\nu - \partial_\nu A_\mu$ is the Maxwell field strength with the vector potential A_μ . In this paper, we use geometric units of $c = G = \hbar = k_B = 1$. The Gauss–Bonnet–AdS black hole can be written as [49–51]

$$ds^2 = -f(r)dt^2 + \frac{dr^2}{f(r)} + r^2[d\theta^2 + \sin^2\theta(d\phi^2 + \sin^2\theta d\psi^2)], \tag{3}$$

in which

$$f(r) = \frac{r^2}{2\alpha} \left(1 - \sqrt{-\frac{4\alpha}{L^2} + \frac{32\alpha M}{3\pi r^4} - \frac{16\alpha Q^2}{3\pi^2 r^6} + 1} \right) + 1, \tag{4}$$

where M is the mass and Q is the charge of the black hole. In the low energy effective action of heterotic string theory, α is proportional to the inverse string tension with positive parameter. Thus in this paper we will consider the case $\alpha > 0$ [36,52]. In addition, from (4), one can see that there is an upper bound for the Gauss–Bonnet parameter, namely $\alpha < L^2/4$.

In the Gauss–Bonnet–AdS background, the black hole event horizon r_h is the largest root of the equation $f(r_h) = 0$. At the event horizon, the Hawking temperature can be expressed as [53]

$$T = \frac{L^2 \left(3\pi^2 r_h^6 \left(\sqrt{\frac{(2\alpha+r_h^2)^2}{r_h^4}} - 1 \right) - 8\alpha Q^2 \right) + 12\pi^2 \alpha r_h^6}{12\pi^3 \alpha L^2 r_h^5 \sqrt{\frac{(2\alpha+r_h^2)^2}{r_h^4}}}, \tag{5}$$

in which we have used the relation

$$M = \frac{4L^2 Q^2 + 3\pi^2 L^2 r_h^4 + 3\pi^2 \alpha L^2 r_h^2 + 3\pi^2 r_h^6}{8\pi L^2 r_h^2}. \tag{6}$$

The chemical potential in this background is

$$\Phi = \frac{Q}{\pi r_h^2}. \tag{7}$$

The entropy of the black hole can be written as

$$S = \frac{\pi^2 r_h^3}{2} \left(\frac{6\alpha}{r_h^2} + 1 \right). \tag{8}$$

Inserting (8) into (5), we can get the relation between the temperature and entropy $T(S, Q)$. Next, we will employ this relation to study the phase structure of the Gauss–Bonnet–AdS black hole in the $T - S$ plane.

2.2. Phase transition of thermal entropy

As we know, for a charged AdS black hole, the spacetime undergoes the Van der Waals-like phase transition as the charge changes from a small value to a large value. Especially there is a critical charge, for which the temperature and entropy satisfy the following relation

$$\left(\frac{\partial T}{\partial S} \right)_Q = \left(\frac{\partial^2 T}{\partial S^2} \right)_Q = 0. \tag{9}$$

In our background, the function $T(S, Q)$ is too prolix so that we are hard to get the analytical value of the critical charge. We will get the critical charge numerically. In the Gauss–Bonnet gravity, it has been found that not only the charge but also the Gauss–Bonnet parameter will affect the phase structure of the black hole. When we discuss the effect of α on the phase structure, the symbol Q in (9) should be replaced by α .

In order to obtain an analogy with the liquid–gas phase transition in fluids, we can identify free energy F of black hole with the Gibbs free energy $G = G(P, V)$ of the fluid, where the P, V correspond to pressure and volume of fluid. In [3], the authors identify cosmology constant and curvature in black hole as pressure and volume to study analogy thermal dynamics. In [3], $(T, S), (\Phi, Q)$ and (V, P) are interpreted as conjugated variables in AdS black system. For our case, one can turn off α to obtain the AdS black hole system studied in [3]. In order to avoid the confusion, we choose two kinds of identifications shown in (10).

Analogy		
Fluid	Gauss–Bonnet AdS black hole	Gauss–Bonnet AdS black hole
Temperature	Q	α
Pressure, P	$T(\alpha)$	$T(Q)$
Volume, V	$S(\alpha)$	$S(Q)$

(10)

It should be stressed that though the Van der Waals-like phase transition can be constructed by transposing intensive with extensive variables with the help of (10), the fluid analogy of the Gauss–Bonnet–AdS black hole in our paper is incomplete. We should emphasize that the complete understanding of the fluid analogy and exact definition of extensive variables are given in [3]. More precisely, in [3], the cosmological constant is treated as a thermodynamic pressure and its conjugate quantity as a thermodynamic volume. The complete fluid analogy has been presented in [3]. In later part of this paper, we are mainly interested in the relation between the thermodynamic entropy and entanglement entropy. Thus it is convenient to discuss the

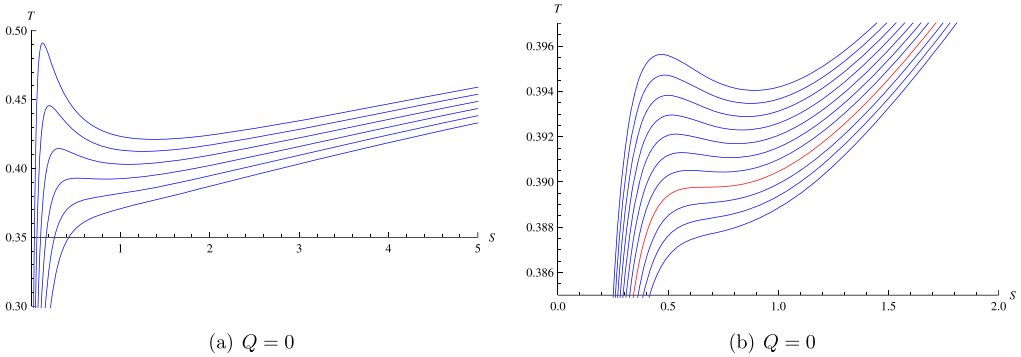


Fig. 1. Relations between entropy and temperature for different α with a fixed Q . In (a), curves from top to down correspond to cases when α varies from 0.015 to 0.035 with step 0.004, while in (b) these curves correspond to cases when α varies from 0.0264 to 0.0284 with step 0.0002. (For interpretation of the references to color in this figure, the reader is referred to the web version of this article.)

Van der Waals-like phase transition in the $T - S$ plane and we can compare the phase structure of thermodynamic entropy and entanglement entropy transparently.

Firstly, we will fix the charge to discuss how the Gauss–Bonnet parameter affects the phase structure. We will set $L = 1$. For the case $Q = 0$, we know that in the Einstein gravity, the black hole undergoes the Hawking–Page transition. But in our background, we find the black hole undergoes the Van der Waals-like phase transition, which is shown in (a) of Fig. 1.

Exactly, to get the Van der Waals-like phase transition in this case, we should find a critical value of the Gauss–Bonnet parameter. For the function $T(S, Q)$ is too prolix, we will get it numerically. We plot a series of curves with taking different values of α in the $T - S$ plane shown in (a) of Fig. 1, and one can read off the region of critical value of the Gauss–Bonnet parameter α which satisfies the condition $(\frac{\partial T}{\partial S})_{\alpha} = 0$. We plot a bunch of curves in the $T - S$ plane with smaller step so that we can get the precise critical value of α . From (b) of Fig. 1, we find the exact critical value of the Gauss–Bonnet parameter should be about 0.0278, which is labeled by the red dashed lines in (b) of Fig. 1. Finally, we adjust the value of α by hand to find the exact value of α that satisfies $(\frac{\partial T}{\partial S})_{\alpha} = 0$, which produces $\alpha_c = 0.0277925$. Adapting the same strategy, we also can get the critical value of the Gauss–Bonnet parameter for the case $Q = 0.1$, which produces $\alpha_c = 0.01972$. The phase structure for a fixed Q is plotted in Fig. 2. As α is fixed, we also can investigate how the charge affects the phase structure of the black hole. For the case $\alpha = 0.01$ and $\alpha = 0.02$, the critical charge Q_c is found to be 0.1681103 and 0.094984 respectively (Fig. 3). The phase structure for a fixed α is plotted in Fig. 4.

From Fig. 2 and Fig. 4, we know that these phase structures are similar to that of the Van der Waals phase structure. That is, the black hole endowed with different charges or Gauss–Bonnet parameters has different phase structures. As the value of the charge or Gauss–Bonnet parameter is smaller than the corresponding critical value, there is a three special phases region where a small black hole, large black hole and an intermediate black hole coexist. From data about T_f Table 1, one can see T_f will increase with increasing charge Q with fixing α (α with fixing Q) to the critical T_c . When $T_f < T_c$, the small black hole will coexist with large black hole. One can make use of equal area law to determined T_f which is the temperature of coexistence of small black hole and large black hole. While the temperature increases to T_c , the swallow tails will shrink to a critical point and equal area will go to vanishing. The large black hole and small black hole will go to one black hole. This phenomenon will be analogous with the one in

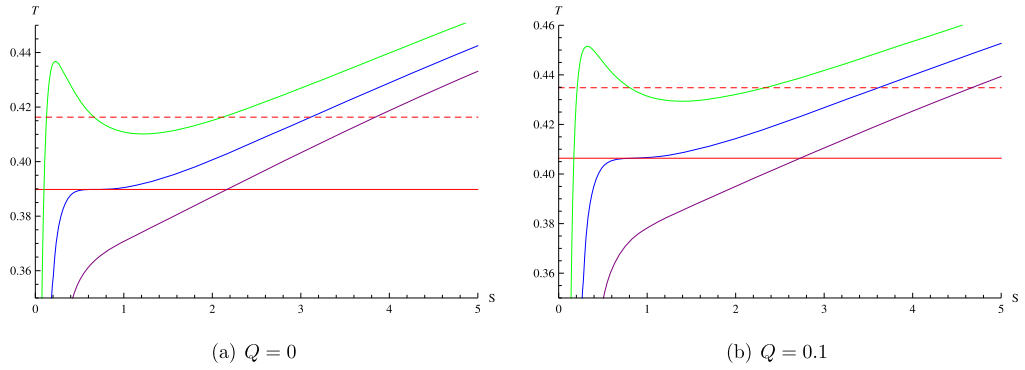


Fig. 2. Relations between entropy and temperature for different α with a fixed Q . In (a), curves from top to down correspond to $\alpha = 0.02, 0.0277925, 0.035$, and in (b) they correspond to $\alpha = 0.01, 0.01972, 0.03$ respectively. The red dashed line and solid line correspond to the first order phase transition temperature T_f and second order phase transition temperature T_c . (For interpretation of the references to color in this figure legend, the reader is referred to the web version of this article.)

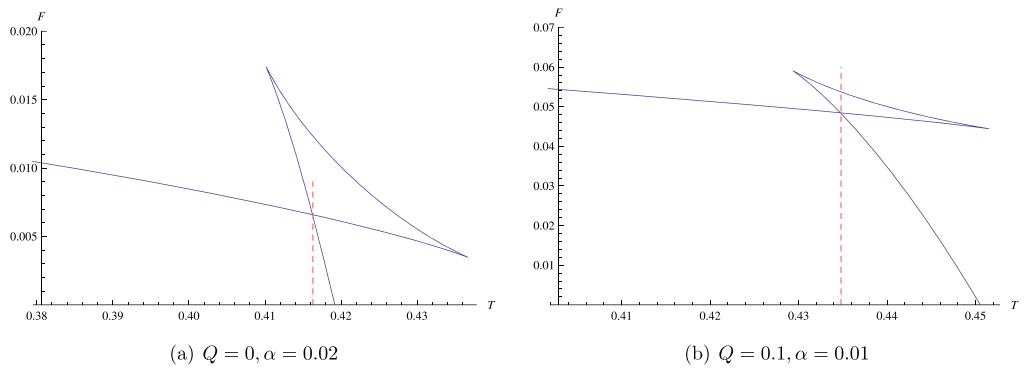


Fig. 3. Relations between the free energy and temperature.

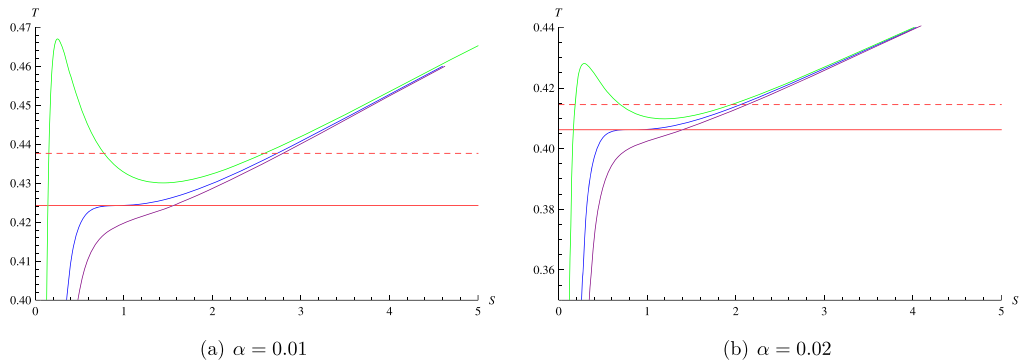


Fig. 4. Relations between entropy and temperature for different Q with a fixed α . In (a), curves from top to down correspond to $Q = 0.08, 0.1681103, 0.2$, and in (b) they correspond to $Q = 0.03, 0.094984, 0.13$ respectively. The red dashed line and solid line correspond to the first order phase transition temperature T_f and second order phase transition temperature T_c . (For interpretation of the references to color in this figure legend, the reader is referred to the web version of this article.)

Table 1

Check of the equal area law in the $T - S$ plane, where the relative error is defined by $\frac{A_L - A_R}{A_R}$.

	T_f	S_{min}	S_{max}	A_L	A_R	Relative error
$Q = 0$	0.4163	0.126349	2.11603	0.828192	0.828303	0.134%
$Q = 1$	0.4348	0.209455	2.32746	0.920752	0.920907	0.169%
$\alpha = 0.01$	0.4377	0.152951	2.59566	1.06919	1.06917	0.018%
$\alpha = 0.2$	0.4145	0.184371	1.95317	0.733093	0.733169	0.010%

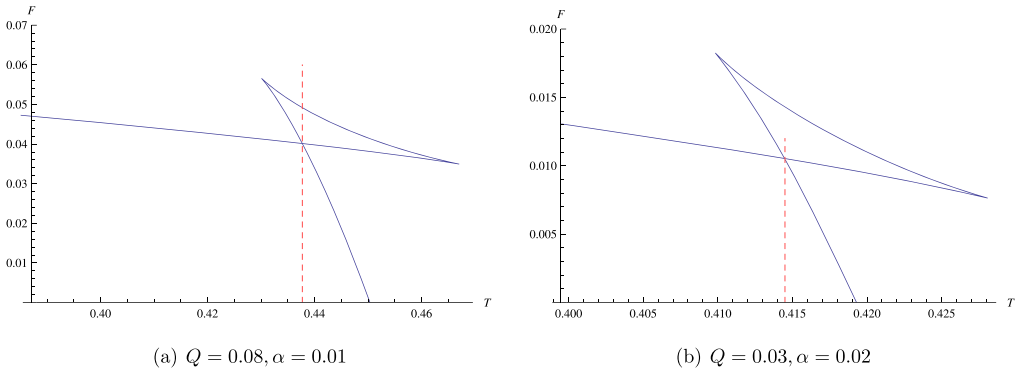


Fig. 5. Relations between the free energy and temperature.

Van der Waals fluid below the critical temperature, as the volume decreased a certain pressure is reached in which gas and liquid coexist. In our case, we can map small black hole and large black hole to liquid phase and gas phase in fluid system in analogy sense. With increasing the value of the charge or Gauss–Bonnet parameter to the corresponding critical value, the small black hole and the large black hole will merge into one and squeeze out the unstable phase such that an inflection point emerges. In this situation, the divergence of the heat capacity implies that there is a second order phase transition. For the case that the value of the charge or Gauss–Bonnet parameter exceeds the corresponding critical value, the black hole is always stable.

The phase structures can also be observed in the $F - T$ plane, in which $F = M - TS$ is the Helmholtz free energy, and M is black hole mass. The pictures for different Q, α are shown in Fig. 3 and Fig. 5. We take the case $Q = 0.03, \alpha = 0.02$ as an example to elaborate their relation. From (b) of Fig. 5, we find there is a swallowtail structure, which corresponds to the unstable phase in the top curve in (b) Fig. 4. The transition temperature $T_f = 0.4145$ is apparently the value of the horizontal coordinate of the junction between the small black hole and the large black hole. When the temperature is lower than the transition temperature T_f , the free energy of the small black hole is lowest which means the small hole is stable and dominant. As the temperature is higher than T_f , the free energy of the large black hole is lowest, so the large black hole dominates thereafter. The non-smoothness of the junction in Fig. 5 indicates that the phase transition is first order.

In addition, the critical temperature T_f also satisfies Maxwell’s equal area law

$$A_L \equiv \int_{S_1}^{S_3} T(S, Q) dS = T_f(S_3 - S_1) \equiv A_R, \tag{11}$$

in which $T(S, Q)$ is the analytical function mentioned above, S_1 and S_3 are the smallest and largest roots of the equation $T(S, Q) = T_f$. For different Q and α , the results are listed in Table 1. From this table, we find A_L equals to A_R within our numerical accuracy. So the equal area law still holds in the $T - S$ plane.

For the second order phase transition in Fig. 2 and Fig. 4, we know that near the critical temperature T_c , there is always a relation [14]

$$\log |T - T_c| = 3 \log |S - S_c| + \text{constant}, \tag{12}$$

in which S_c is the critical entropy corresponding to the critical temperature. With the definition of the heat capacity

$$C_Q = T \left. \frac{\partial S}{\partial T} \right|_Q, \tag{13}$$

one can get further $C_Q \sim (T - T_c)^{-2/3}$, namely the critical exponent is $-2/3$, which is the same as the one [54] from the mean field theory. Next, we will check whether there is a similar relation as (12) to check the critical exponent of the heat capacity in the framework of holography.

3. Phase structure of the non-local observables

Having understood the phase structure of the black hole from the viewpoint of thermodynamics, we will employ the non-local observables such as holographic entanglement entropy, Wilson loop, and two point correlation function to probe the phase structure. The main motivation is to check whether the non-local observables exhibit the similar phase structure as that of the thermal entropy.

3.1. Phase structure probed by holographic entanglement entropy

The holographic entanglement entropy in the Gauss–Bonnet gravity can be proposed as [39–46]

$$S_A = \frac{2\pi}{\ell_p^3} \int_M d^3x \sqrt{h} \left[1 + \alpha L^2 \mathcal{R} \right] + \frac{4\pi}{\ell_p^3} \int_{\partial M} d^2x \sqrt{h} \alpha L^2 \mathcal{K}. \tag{14}$$

The first integral in (14) is evaluated on the bulk surface M , the second one is on boundary ∂M , which is the boundary of M regularized at $r = r_0$, \mathcal{R} is the Ricci scalar for the intrinsic metric of M , \mathcal{K} is the trace of the extrinsic curvature of the boundary of M and h is the determinant of the induced metric on M . The second term in the first integral (14) is present due to higher derivative gravity appeared in the background. The minimal value of the functional (14) would give the entanglement entropy of the subsystem A .

For our background, the entangling surface is parameterized as a constant θ hypersurface $\theta = \theta_0$ with coordinates $0 \leq \phi \leq \pi, 0 \leq \psi \leq 2\pi$. In this case, based on (14), we can get the equation of motion of $r(\theta)$

$$\begin{aligned} &\pi^2 r(\theta) (r'(\theta))^2 (\sin(\theta) r(\theta))^2 f'(r(\theta)) - 2 \cos(\theta) r'(\theta) - 2r(\theta) f(r(\theta)) (r(\theta) (\sin(\theta) r''(\theta) \\ &- 3 + \cos(\theta) r'(\theta) \sin(\theta) r'(\theta)^2) + 4 \sin(\theta) r(\theta)^3 f(r(\theta))^2) = 0, \end{aligned} \tag{15}$$

in which $r' = dr/d\theta$. To solve this equation, we will resort to the following boundary conditions

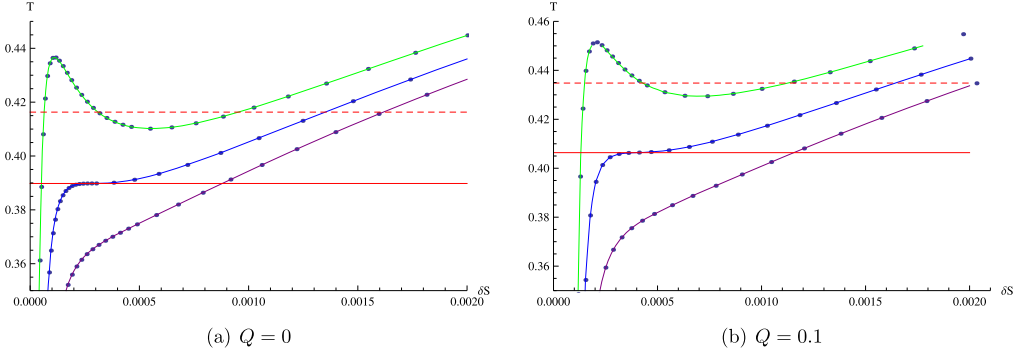


Fig. 6. Relations between holographic entanglement entropy and temperature for different α at a fixed Q . In (a), curves from top to down correspond to $\alpha = 0.02, 0.0277925, 0.035$, and in (b) they correspond to $\alpha = 0.01, 0.01972, 0.03$ respectively. The red dashed line and solid line correspond to the first order phase transition temperature T_f and second order phase transition temperature T_c . (For interpretation of the references to color in this figure legend, the reader is referred to the web version of this article.)

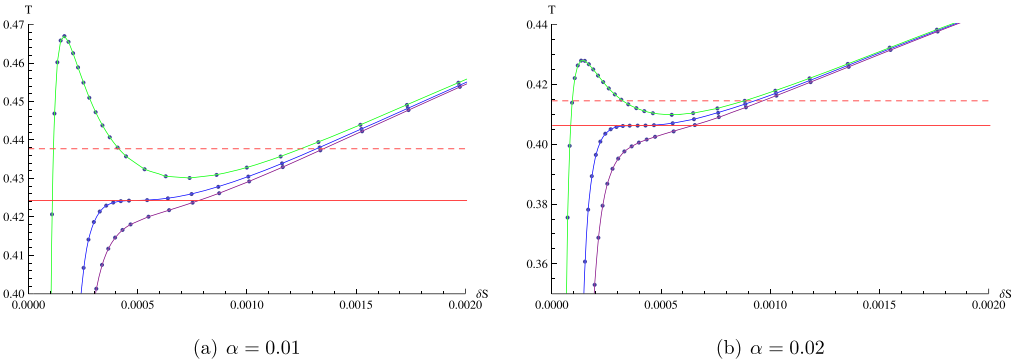


Fig. 7. Relations between holographic entanglement entropy and temperature for different Q at a fixed α . In (a), curves from top to down correspond to $Q = 0.08, 0.1681103, 0.2$, and in (b) they correspond to $Q = 0.03, 0.094984, 0.13$ respectively. The red dashed line and solid line correspond to the first order phase transition temperature T_f and second order phase transition temperature T_c . (For interpretation of the references to color in this figure legend, the reader is referred to the web version of this article.)

$$r'(0) = 0, r(0) = r_0. \tag{16}$$

In addition, to avoid the entanglement entropy to be contaminated by the surface that wraps the horizon, we will choose a small region A as in [14]. In this paper, we will choose $\theta_0 = 0.2$. Note that for a fixed θ_0 , the entanglement entropy is divergent, so it should be regularized by subtracting off the entanglement entropy in pure AdS with the same boundary region, denoted by S_0 . To achieve this, we are required to set a UV cutoff, which is chosen to be $r_0 = r(0.199)$. The regularized entanglement entropy is labeled as $\delta S \equiv S_A - S_0$.

With these assumptions, we can plot the phase structure of entanglement entropy for a fixed charge Q or a fixed Gauss–Bonnet parameter α , which are shown in Fig. 6 and Fig. 7. It is obvious that Fig. 6 and Fig. 7 resemble Fig. 2 and Fig. 4 respectively. Especially, the first order phase transition temperature T_f and second order phase transition temperature T_c are exactly the same as that in the $T - S$ plane. We will employ the equal area law to locate the first order phase

Table 2

Check of the equal area law in the $T - \delta S$ plane, where the relative error is defined by $\frac{A_L - A_R}{A_R}$.

	T_f	δS_{min}	δS_{max}	A_L	A_R	Relative error
$Q = 0$	0.4163	0.00006408	0.0009523	0.00036975	0.00036984	0.02466%
$Q = 0.1$	0.4348	0.0001495	0.001124	0.00042361	0.00042367	0.01496%
$\alpha = 0.01$	0.4377	0.0001149	0.0012467	0.00049540	0.00049571	0.06335%
$\alpha = 0.02$	0.4145	0.00009349	0.0008822	0.00032692	0.00032696	0.01147%

transition temperature, and critical exponent of the analogous heat capacity to locate the second order phase transition temperature.

Similar to (11), the equal area law in $T - \delta S$ plane can be defined as

$$A_L \equiv \int_{\delta S_{min}}^{\delta S_{max}} T(\delta S, Q) d\delta S = T_f(\delta S_{max} - \delta S_{min}) \equiv A_R, \quad (17)$$

in which $T(\delta S)$ is an interpolating function obtained from the numeric data, T_f is the phase transition temperature, and δS_{min} , δS_{max} are the smallest and largest values of the equation $T(\delta S) = T_f$. For different Q and α , the calculated results are listed in Table 2. From this table, we can see that for the unstable region of the first order phase transition in the $T - \delta S$ plane, the equal area law holds within our numeric accuracy.

In order to investigate the critical exponent of the second order phase transition in the $T - \delta S$ plane, we define an analogous heat capacity

$$C = T \frac{\partial \delta S}{\partial T}. \quad (18)$$

Provided a similar relation as shown in (12) is satisfied, one can get the critical exponent of the analogous heat capacity immediately. So next, we are interested in the logarithm of the quantities $T - T_c$, $\delta S - \delta S_c$, in which T_c is the second order phase transition temperature, and δS_c is obtained numerically by the equation $T(\delta S) = T_c$. The relations between $\log |T - T_c|$ and $\log |\delta S - \delta S_c|$ for different Q and α are shown in Fig. 8. By data fitting, the straight lines in Fig. 8 can be expressed as

$$\log |T - T_c| = \begin{cases} 20.3652 + 3.00026 \log |\delta S - \delta S_c|, & \text{for } Q = 0, \alpha = 0.0277925, \\ 20.668 + 3.0015 \log |\delta S - \delta S_c|, & \text{for } Q = 0.1, \alpha = 0.01972, \\ 20.817 + 3.00773 \log |\delta S - \delta S_c|, & \text{for } Q = 0.1681103, \alpha = 0.01, \\ 20.8815 + 3.08132 \log |\delta S - \delta S_c|, & \text{for } Q = 0.094984, \alpha = 0.02. \end{cases} \quad (19)$$

It is obvious that for all the lines, the slope is about 3, which resembles that in (12). That is, the critical exponent of the analogous heat capacity in $T - \delta S$ plane is the same as that in the $T - S$ plane, which once reinforce the conclusion that the phase structure of the entanglement entropy is the same as that of the thermal entropy.

3.2. Phase structure probed by Wilson loop

In this subsection, we will employ the Wilson loop to probe the phase structure of the Gauss–Bonnet–AdS black hole. According to the AdS/CFT correspondence, the expectation value of the Wilson loop is related to the string partition function

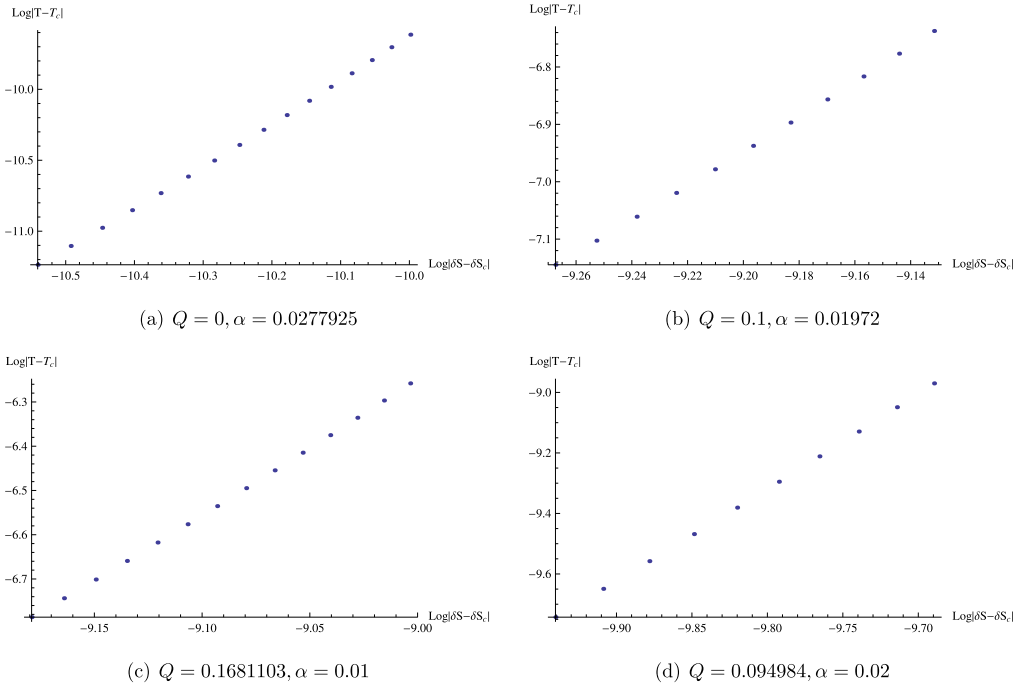


Fig. 8. Relations between $\log |T - T_c|$ and $\log |\delta S - \delta S_c|$ for different Q and α .

$$\langle W(C) \rangle = \int D\Sigma e^{-A(\Sigma_0)}, \tag{20}$$

in which C is the closed contour, Σ_0 is the string world sheet which extends in the bulk with the boundary condition $\partial \Sigma_0 = C$, and $A(\Sigma_0)$ corresponds to the Nambu–Goto action for the string. In the strongly coupled limit, we can simplify the computation by making a saddle point approximation and evaluating the minimal area surface of the classical string with the same boundary condition $\partial \Sigma_0 = C$, which leads to [55]

$$\langle W(C) \rangle \approx e^{-A(\Sigma)}, \tag{21}$$

where Σ represents the minimal area surface. Next we choose the line with $\phi = \frac{\pi}{2}$ and $\theta = \theta_0$ as our loop. Then we can employ (θ, ψ) to parameterize the minimal area surface, which is invariant under the ψ -direction by our rotational symmetry. Thus the corresponding minimal area surface can be expressed as

$$A = 2\pi \int_0^{\theta_0} r \sin \theta \sqrt{\frac{r'^2}{f(r)} + r^2} d\theta. \tag{22}$$

Similar to the case of entanglement entropy, we will also use the boundary condition in (16) to solve $r(\theta)$ with the choice $\theta_0 = 0.2$. We label the regularized minimal area surface as $\delta A \equiv A - A_0$, where A_0 is the minimal area in pure AdS with the same boundary region. We plot the relation between δA and T for different Q and α in Fig. 9 and Fig. 10. Comparing Fig. 9 and Fig. 10 with Fig. 2 and Fig. 4, we find they are the same nearly besides the scale of the horizontal

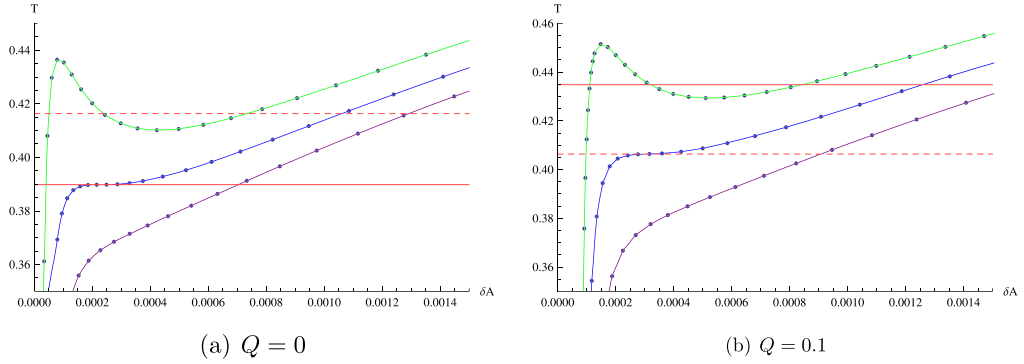


Fig. 9. Relations between minimal area surface and temperature for different α at a fixed Q . In (a), curves from top to down correspond to $\alpha = 0.02, 0.0277925, 0.035$, and in (b) they correspond to $\alpha = 0.01, 0.01972, 0.03$ respectively. The red dashed line and solid line correspond to the first order phase transition temperature T_f and second order phase transition temperature T_c . (For interpretation of the references to color in this figure legend, the reader is referred to the web version of this article.)

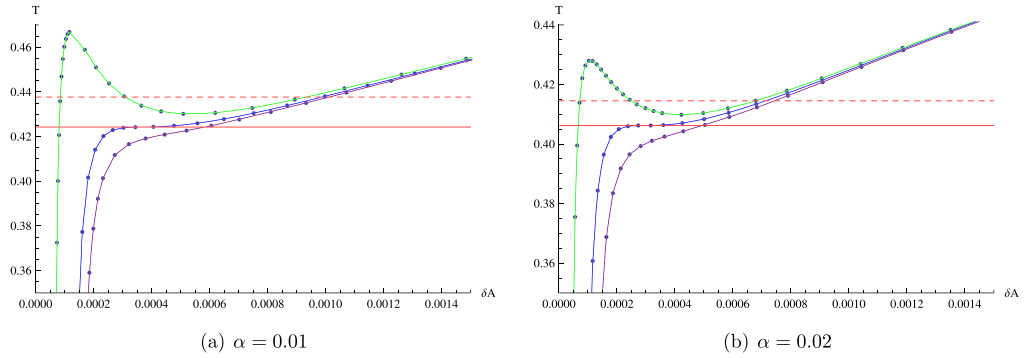


Fig. 10. Relations between minimal area surface and temperature for different Q at a fixed α . In (a), curves from top to down correspond to $Q = 0.08, 0.1681103, 0.2$, and in (b) they correspond to $Q = 0.03, 0.094984, 0.13$ respectively. The red dashed line and solid line correspond to the first order phase transition temperature T_f and second order phase transition temperature T_c . (For interpretation of the references to color in this figure legend, the reader is referred to the web version of this article.)

coordinate. The result tells us that the similar phase structure also shows up for the minimal surface area, which is the same as that of the entanglement entropy.

It is also necessary to check the equal area law for the first order phase transition and critical exponent of the analogous heat capacity for the second order phase transition in the $T - \delta A$ plane. The equal area law in this case can be defined as

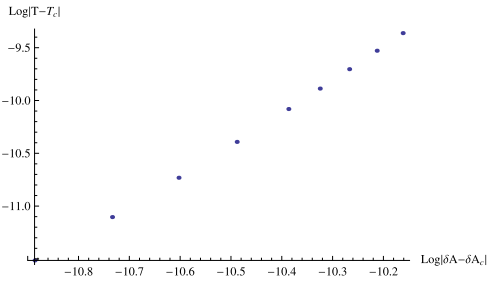
$$A_L \equiv \int_{\delta A_{min}}^{\delta A_{max}} T(\delta A, Q) d\delta A = T_f(\delta A_{max} - \delta A_{min}) \equiv A_R, \tag{23}$$

in which $\delta A_{min}, \delta A_{max}$ are the smallest and largest values of the equation $T(\delta A) = T_f$, where $T(\delta A)$ is an interpolating function obtained by data fitting. For different Q and α , the calculated results are listed in Table 3. Obviously, as that in the $T - \delta S$ plane, the equal area law also holds

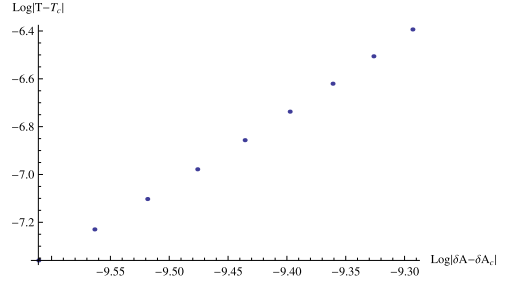
Table 3

Check of the equal area law in the $T - \delta A$ plane, where the relative error is defined by $\frac{A_L - A_R}{A_R}$.

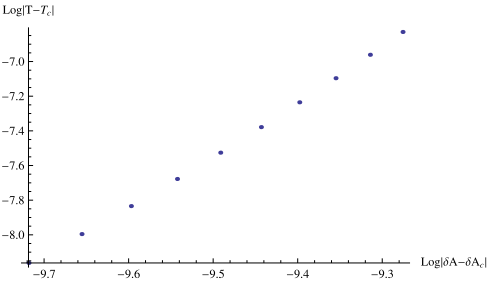
	T_f	δA_{min}	δA_{max}	A_L	A_R	Relative error
$Q = 0$	0.4163	0.00007374	0.0007352	0.0002742	0.0002754	0.4048%
$Q = 0.1$	0.4348	0.0001110	0.0008404	0.0003172	0.0003171	0.008852%
$\alpha = 0.01$	0.4377	0.00006426	0.0009327	0.0003785	0.0003801	0.4285%
$\alpha = 0.02$	0.4145	0.00007167	0.0006778	0.0002513	0.0002512	0.01042%



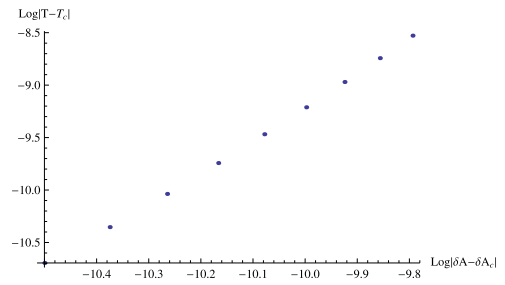
(a) $Q = 0, \alpha = 0.0277925$



(b) $Q = 0.1, \alpha = 0.01972$



(c) $\alpha = 0.01, Q = 0.1681103$



(d) $\alpha = 0.02, Q = 0.094984$

Fig. 11. Relations between $\log |T - T_c|$ and $\log |\delta A - \delta A_c|$ for different Q and α .

within our numeric accuracy, which implies that the minimal area surface owns the same first order phase transition as that of the thermal entropy.

For the second order phase transition, we are interested in the logarithm of the quantities $T - T_c$, $\delta A - \delta A_c$, in which T_c is the second order phase transition temperature, and δA_c is obtained numerically by the equation $T(\delta A) = T_c$. The relations between $\log |T - T_c|$ and $\log |\delta A - \delta A_c|$ for different Q and α are shown in Fig. 11. The straight line in each subgraph can be fitted as

$$\log |T - T_c| = \begin{cases} 20.9318 + 2.98393 \log |\delta A - \delta A_c|, & \text{for } Q = 0, \alpha = 0.0277925, \\ 21.843 + 3.04022 \log |\delta A - \delta A_c|, & \text{for } Q = 0.1, \alpha = 0.01972, \\ 21.1332 + 3.0174 \log |\delta A - \delta A_c|, & \text{for } Q = 0.1681103, \alpha = 0.01, \\ 21.5862 + 3.07862 \log |\delta A - \delta A_c|, & \text{for } Q = 0.094984, \alpha = 0.02. \end{cases} \quad (24)$$

Similar to that of the entanglement entropy, the slope of the fitted straight line is also about 3, which implies that the critical exponent of the analogous heat capacity is $-2/3$ in the $T - \delta A$ plane. This result is consistent with that of the thermal entropy too, which reminds that the minimal area surface exhibits the same second order phase transition as that of the thermal entropy.

3.3. Phase structure probed by two point correlation function

In this subsection, we would like to study a scalar operator \mathcal{O} with large conformal dimension Δ in the dual field theory. Due to the saddle point approximation, the equal time two point correlation function can be written as follows [56]

$$\langle \mathcal{O}(t, x_i) \mathcal{O}(t, x_j) \rangle \approx e^{-\Delta \bar{L}}, \tag{25}$$

in which \bar{L} is the length of the bulk geodesic between the points (t, x_i) and (t, x_j) on the AdS boundary. In our gravity model, we can simply choose $(\phi = \frac{\pi}{2}, \theta = 0, \psi = 0)$ and $(\phi = \frac{\pi}{2}, \theta = \theta_0, \psi = \pi)$ as the two boundary points. Then with θ to parameterize the trajectory, the proper length is given by

$$\bar{L} = \int_0^{\theta_0} \sqrt{\frac{r'^2}{f(r)} + r^2} d\theta. \tag{26}$$

With the boundary condition in (16), we can get the numeric result of $r(\theta)$ and further get \bar{L} by substituting $r(\theta)$ into (26). Similarly, we label the regularized geodesic length as $\delta L \equiv \bar{L} - \bar{L}_0$, where \bar{L}_0 is the geodesic length in pure AdS with the same boundary region. The relations between δL and T for different Q and α are shown in Fig. 12 and Fig. 13. It is obvious that Fig. 12 and Fig. 13 resemble Fig. 2 and Fig. 4 respectively besides the scale of horizontal coordinate, which implies that the geodesic length owns the same phase structure as that of the thermal entropy. Especially they have the same first order phase transition temperature and second order phase transition temperature, which will be checked next by investigating the equal area law for the first order phase transition and critical exponent for the second order phase transition.

In the $T - \delta L$ plane, the equal area law can be defined as

$$A_L \equiv \int_{\delta L_{min}}^{\delta L_{max}} T(\delta L, Q) d\delta L = T_f(\delta L_{max} - \delta L_{min}) \equiv A_R, \tag{27}$$

in which $\delta L_{min}, \delta L_{max}$ are the smallest and largest values of the equation $T(\delta L) = T_f$, where $T(\delta L)$ is also an interpolating function. For different Q and α , the results are listed in Table 4. We can see that in the $T - \delta L$ plane, the equal area law holds within a reasonable numeric accuracy.

For the second order phase transition, we will investigate the relation between $\log |T - T_c|$ and $\log |\delta L - \delta L_c|$ for different Q and α , which are shown in Fig. 14. The straight lines in this figure can be fitted respectively as

$$\log |T - T_c| = \begin{cases} 31.3704 + 3.02888 \log |\delta L - \delta L_c|, & \text{for } Q = 0, \alpha = 0.0277925, \\ 32.1586 + 2.99908 \log |\delta L - \delta L_c|, & \text{for } Q = 0.1, \alpha = 0.01972, \\ 32.4443 + 3.06135 \log |\delta L - \delta L_c|, & \text{for } Q = 0.1681103, \alpha = 0.01, \\ 32.494 + 3.05543 \log |\delta L - \delta L_c|, & \text{for } Q = 0.094984, \alpha = 0.02. \end{cases} \tag{28}$$

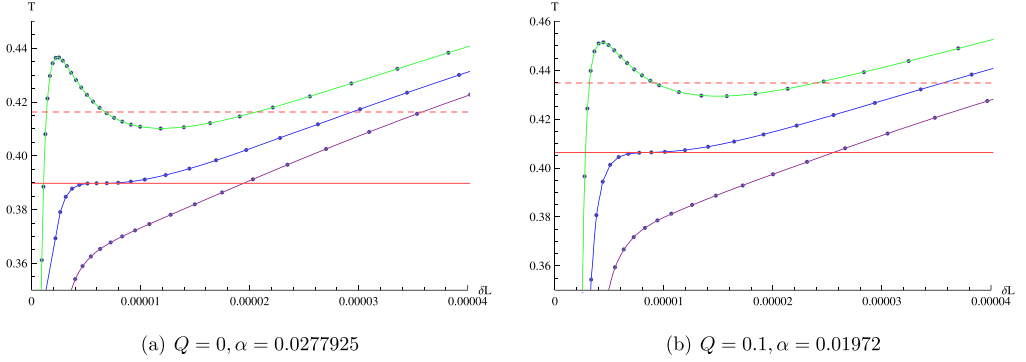


Fig. 12. Relations between geodesic length and temperature for different α at a fixed Q . In (a), curves from top to down correspond to $\alpha = 0.02, 0.0277925, 0.035$, and in (b) they correspond to $\alpha = 0.01, 0.01972, 0.03$ respectively. The red dashed line and solid line correspond to the first order phase transition temperature T_f and second order phase transition temperature T_c . (For interpretation of the references to color in this figure legend, the reader is referred to the web version of this article.)

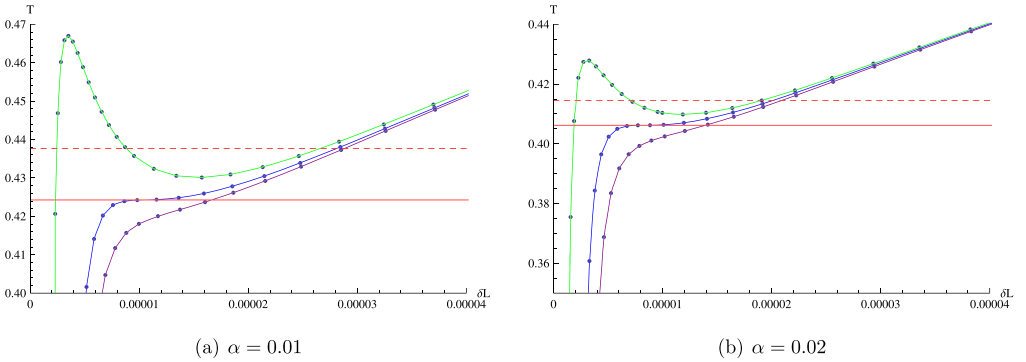


Fig. 13. Relations between geodesic length and temperature for different Q at a fixed α . In (a), curves from top to down correspond to $Q = 0.08, 0.1681103, 0.2$, and in (b) they correspond to $Q = 0.03, 0.094984, 0.13$ respectively. The red dashed line and solid line correspond to the first order phase transition temperature T_f and second order phase transition temperature T_c . (For interpretation of the references to color in this figure legend, the reader is referred to the web version of this article.)

Table 4

Check of the equal area law in the $T - \delta L$ plane, where the relative error is defined by $\frac{A_L - A_R}{A_R}$.

	T_f	δL_{min}	δL_{max}	A_L	A_R	Relative error
$Q = 0$	0.4163	2.1207×10^{-6}	0.00002072	7.7104×10^{-6}	7.7418×10^{-6}	0.4058%
$Q = 0.1$	0.4348	3.2756×10^{-6}	0.00002398	9.0415×10^{-6}	9.0402×10^{-6}	0.0147%
$\alpha = 0.01$	0.4377	2.0984×10^{-6}	0.00002661	0.00001051	0.000010727	1.9899%
$\alpha = 0.02$	0.4145	1.3642×10^{-6}	0.00001894	7.3222×10^{-6}	7.2869×10^{-6}	0.4820%

It is obvious that the slope of the fitted straight line is also about 3, which implies that the critical exponent of the analogous heat capacity is $-2/3$ in the $T - \delta L$ plane. The phase structures shown by equal time two heavy operators correlation function are consistent with that given by the holographic entanglement entropy and expectation value of Wilson loop.

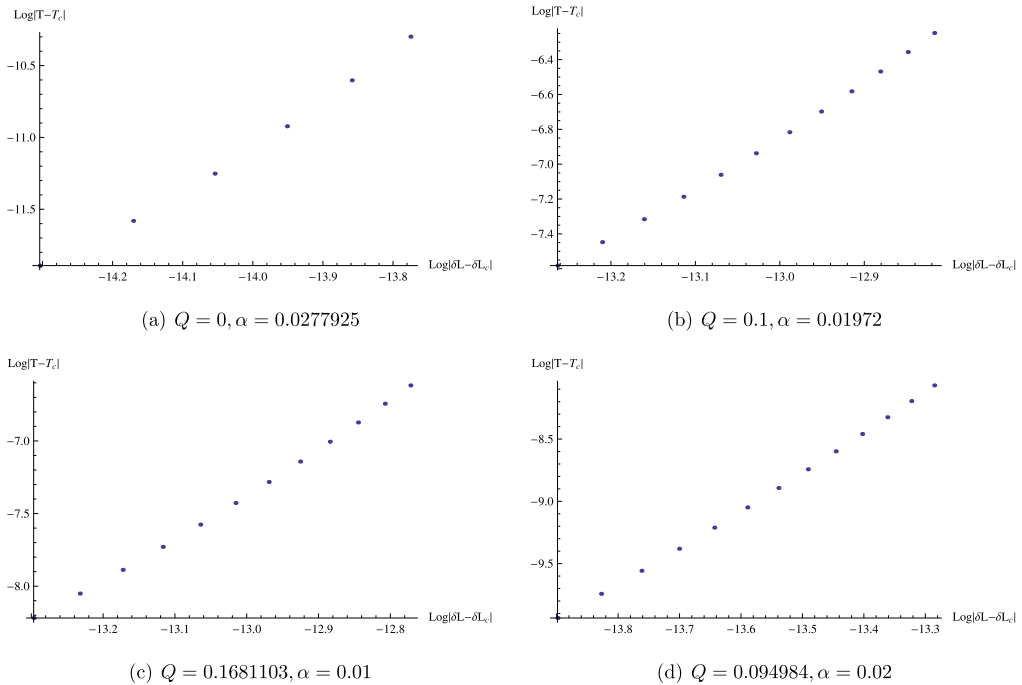


Fig. 14. Relations between $\log |T - T_c|$ and $\log |\delta L - \delta L_c|$ for different Q and α .

4. Conclusions

In this paper, we have studied the thermal entropy of a (4+1)-dimensional spherical Gauss–Bonnet–AdS black hole and found that there is van der Waals-like phase transition in the $T - S$ plane for a fixed charge Q or a fixed Gauss–Bonnet parameter α . For the case $Q = 0$, the neutral spherical Gauss–Bonnet–AdS black hole still undergoes the van der Waals-like phase transition rather than the Hawking–Page phase transition appeared in the Einstein gravity, which have been studied intensively.

For spherical AdS black hole in Einstein gravity, [14] has observed that holographic entanglement entropy will also undergo van der Waals-like phase transition which is much analogous to that in thermal entropy. We extended this observation to (4+1)-dimensional spherical Gauss–Bonnet–AdS black hole and found there is a similar phenomenon. We apply AdS/CFT to study some non-local observables such as holographic entanglement entropy, Wilson loop, and two point correlation function, which are dual to the minimal volume, minimal area, and geodesic length respectively in the conformal field theory. For a fixed charge or a fixed Gauss–Bonnet parameter, all these quantities show that there exist van der Waals-like phase transitions, which happen in thermal entropy already. Below the critical charge or critical Gauss–Bonnet parameter, there exists phase which is composed by a small black hole, large black hole and an intermediate black hole. In this phase, the intermediate black hole will be not stable and the small black hole will directly jump to the large black hole as the temperature increases to the first order phase transition temperature T_f . More precisely, we checked Maxwell’s equal area law and found it was valid for all the charges and Gauss–Bonnet parameters to confirm the first order phase transition. As the value of the charge or Gauss–Bonnet parameter increases to the critical value, the small

black hole and the large black hole merges into one and the intermediate black hole disappears at transition temperature T_c . For this case, phase transition will be the second order. The critical exponent of the analogous heat capacity is found to be consistent with that of the mean field theory. The black hole is always stable as the value of the charge or Gauss–Bonnet parameter is larger than the critical value. Our results confirm the fact that all the nonlocal quantities exhibit van der Waals-like phase transitions in the dual field theory regardless of the dual gravity model.

Acknowledgements

We would like to thank Rong-Gen Cai for his discussions. S.H. is supported by Max-Planck fellowship in Germany and the National Natural Science Foundation of China (No. 11305235). L.L. is supported by the National Natural Science Foundation of China (Grant No. 11575270). X.Z. is supported by the National Natural Science Foundation of China (Grant No. 11405016), China Postdoctoral Science Foundation (Grant No. 2016M590138), Natural Science Foundation of Education Committee of Chongqing (Grant No. KJ1500530), and Basic Research Project of Science and Technology Committee of Chongqing (Grant No. cstc2016jcyjja0364).

References

- [1] A. Chamblin, R. Emparan, C.V. Johnson, R.C. Myers, Charged AdS black holes and catastrophic holography, *Phys. Rev. D* 60 (1999) 064018, arXiv:hep-th/9902170.
- [2] C. Niu, Y. Tian, X.N. Wu, Critical phenomena and thermodynamic geometry of RN–AdS black holes, *Phys. Rev. D* 85 (2012) 024017, arXiv:1104.3066 [hep-th].
- [3] D. Kubiznak, R.B. Mann, P–V criticality of charged AdS black holes, *J. High Energy Phys.* 1207 (2012) 033, arXiv:1205.0559 [hep-th].
- [4] J. Xu, L.M. Cao, Y.P. Hu, P–V criticality in the extended phase space of black holes in massive gravity, *Phys. Rev. D* 91 (2015) 124033, arXiv:1506.03578 [gr-qc].
- [5] R.G. Cai, Y.P. Hu, Q.Y. Pan, Y.L. Zhang, Thermodynamics of black holes in massive gravity, *Phys. Rev. D* 91 (2015) 024032, arXiv:1409.2369 [hep-th].
- [6] S.H. Hendi, A. Sheykhi, S. Panahiyan, B. Eslam Panah, Phase transition and thermodynamic geometry of Einstein–Maxwell–dilaton black holes, *Phys. Rev. D* 92 (2015) 064028, arXiv:1509.08593 [hep-th].
- [7] R.A. Hennigar, W.G. Brenna, R.B. Mann, P–V criticality in quasitopological gravity, *J. High Energy Phys.* 1507 (2015) 077, arXiv:1505.05517 [hep-th].
- [8] S.W. Wei, Y.X. Liu, Clapeyron equations and fitting formula of the coexistence curve in the extended phase space of charged AdS black holes, *Phys. Rev. D* 91 (2015) 044018, arXiv:1411.5749 [hep-th].
- [9] J.X. Mo, W.B. Liu, P–V criticality of topological black holes in Lovelock–Born–Infeld gravity, *Eur. Phys. J. C* 74 (2014) 2836, arXiv:1401.0785 [hep-th].
- [10] E. Spallucci, A. Smailagic, Maxwell’s equal area law for charged Anti-de Sitter black holes, *Phys. Lett. B* 723 (2013) 436, arXiv:1305.3379 [hep-th].
- [11] J.M. Maldacena, Large N limit of superconformal field theories and supergravity, *Int. J. Theor. Phys.* 38 (1999) 1113.
- [12] E. Witten, Anti-de Sitter space and holography, *Adv. Theor. Math. Phys.* 2 (1998) 253, arXiv:hep-th/9802150.
- [13] S.S. Gubser, I.R. Klebanov, A.M. Polyakov, Gauge theory correlators from noncritical string theory, *Phys. Lett. B* 428 (1998) 105, arXiv:hep-th/9802109.
- [14] C.V. Johnson, Large N phase transitions, finite volume, and entanglement entropy, *J. High Energy Phys.* 1403 (2014) 047, arXiv:1306.4955 [hep-th].
- [15] S. Ryu, T. Takayanagi, Holographic derivation of entanglement entropy from AdS/CFT, *Phys. Rev. Lett.* 96 (2006) 181602, arXiv:hep-th/0603001.
- [16] S. Ryu, T. Takayanagi, Aspects of holographic entanglement entropy, *J. High Energy Phys.* 0608 (2006) 045, arXiv:hep-th/0605073.
- [17] P.H. Nguyen, An equal area law for the van der Waals transition of holographic entanglement entropy, *J. High Energy Phys.* 12 (2015) 139, arXiv:1508.01955 [hep-th].

- [18] E. Caceres, P.H. Nguyen, J.F. Pedraza, Holographic entanglement entropy and the extended phase structure of STU black holes, *J. High Energy Phys.* 1509 (2015) 184, arXiv:1507.06069 [hep-th].
- [19] X.X. Zeng, H. Zhang, L.F. Li, Phase transition of holographic entanglement entropy in massive gravity, *Phys. Lett. B* 756 (2016) 170, arXiv:1511.00383 [gr-qc].
- [20] X.X. Zeng, L.F. Li, Van der Waals phase transition in the framework of holography, arXiv:1512.08855 [gr-qc].
- [21] X.X. Zeng, X.M. Liu, L.F. Li, Phase structure of the Born–Infeld–Anti-de Sitter black holes probed by non-local observables, arXiv:1601.01160 [gr-qc].
- [22] A. Dey, S. Mahapatra, T. Sarkar, Thermodynamics and entanglement entropy with Weyl corrections, arXiv:1512.07117 [hep-th].
- [23] J.X. Mo, G.Q. Li, Z.T. Lin, X.X. Zeng, Van der Waals like behavior and equal area law of two point correlation function of $f(R)$ AdS black holes, arXiv:1604.08332 [gr-qc].
- [24] D. Li, S. He, M. Huang, Q.S. Yan, Thermodynamics of deformed AdS₅ model with a positive/negative quadratic correction in graviton–dilaton system, *J. High Energy Phys.* 1109 (2011) 041, arXiv:1103.5389 [hep-th].
- [25] R.G. Cai, S. He, D. Li, A hQCD model and its phase diagram in Einstein–Maxwell–dilaton system, *J. High Energy Phys.* 1203 (2012) 033, arXiv:1201.0820 [hep-th].
- [26] R.G. Cai, S. He, L. Li, Y.L. Zhang, Holographic entanglement entropy in insulator/superconductor transition, *J. High Energy Phys.* 1207 (2012) 088, [http://dx.doi.org/10.1007/JHEP07\(2012\)088](http://dx.doi.org/10.1007/JHEP07(2012)088), arXiv:1203.6620 [hep-th].
- [27] R.G. Cai, S. He, L. Li, Y.L. Zhang, Holographic entanglement entropy on P-wave superconductor phase transition, *J. High Energy Phys.* 1207 (2012) 027, arXiv:1204.5962 [hep-th].
- [28] R.G. Cai, S. He, L. Li, L.F. Li, Entanglement entropy and Wilson loop in Stückelberg holographic insulator/superconductor model, *J. High Energy Phys.* 1210 (2012) 107, arXiv:1209.1019 [hep-th].
- [29] V. Balasubramanian, et al., Thermalization of strongly coupled field theories, *Phys. Rev. Lett.* 106 (2011) 191601, arXiv:1012.4753 [hep-th].
- [30] V. Balasubramanian, et al., Holographic thermalization, *Phys. Rev. D* 84 (2011) 026010, arXiv:1103.2683 [hep-th].
- [31] D. Galante, M. Schvellinger, Thermalization with a chemical potential from AdS spaces, *J. High Energy Phys.* 1207 (2012) 096, arXiv:1205.1548 [hep-th].
- [32] E. Caceres, A. Kundu, Holographic thermalization with chemical potential, *J. High Energy Phys.* 1209 (2012) 055, arXiv:1205.2354 [hep-th].
- [33] X.X. Zeng, D.Y. Chen, L.F. Li, Holographic thermalization and gravitational collapse in the spacetime dominated by quintessence dark energy, *Phys. Rev. D* 91 (2015) 046005, arXiv:1408.6632 [hep-th].
- [34] H. Liu, S.J. Suh, Entanglement Tsunami: universal scaling in holographic thermalization, *Phys. Rev. Lett.* 112 (2014) 011601, arXiv:1305.7244 [hep-th].
- [35] S.J. Zhang, E. Abdalla, Holographic thermalization in charged dilaton Anti-de Sitter spacetime, *Nucl. Phys. B* 896 (2015) 569, arXiv:1503.07700 [hep-th].
- [36] A. Buchel, R.C. Myers, A.v. Niekerk, Nonlocal probes of thermalization in holographic quenches with spectral methods, *J. High Energy Phys.* 02 (2015) 017, arXiv:1410.6201 [hep-th].
- [37] B. Craps, et al., Gravitational collapse and thermalization in the hard wall model, *J. High Energy Phys.* 02 (2014) 120, arXiv:1311.7560 [hep-th].
- [38] G. Camilo, B. Cuadros-Melgar, E. Abdalla, Holographic thermalization with a chemical potential from Born–Infeld electrodynamics, *J. High Energy Phys.* 02 (2015) 103, arXiv:1412.3878 [hep-th].
- [39] J. de Boer, M. Kulaxizi, A. Parnachev, Holographic entanglement entropy in Lovelock gravities, *J. High Energy Phys.* 1107 (2011) 109, arXiv:1101.5781 [hep-th].
- [40] L.-Y. Hung, R.C. Myers, M. Smolkin, On holographic entanglement entropy and higher curvature gravity, *J. High Energy Phys.* 1104 (2011) 025, arXiv:1101.5813 [hep-th].
- [41] D.V. Fursaev, Proof of the holographic formula for entanglement entropy, *J. High Energy Phys.* 0609 (2006) 018, arXiv:hep-th/0606184.
- [42] N. Ogawa, T. Takayanagi, Higher derivative corrections to holographic entanglement entropy for AdS solitons, *J. High Energy Phys.* 1110 (2011) 147, arXiv:1107.4363 [hep-th].
- [43] R.C. Myers, A. Sinha, Seeing a c-theorem with holography, *Phys. Rev. D* 82 (2010) 046006, arXiv:1006.1263 [hep-th].
- [44] X. Dong, Holographic entanglement entropy for general higher derivative gravity, *J. High Energy Phys.* 1401 (2014) 044, arXiv:1310.5713 [hep-th].
- [45] J. Camps, Generalized entropy and higher derivative gravity, *J. High Energy Phys.* 1403 (2014) 070, arXiv:1310.6659 [hep-th].
- [46] R.X. Miao, W.z. Guo, Holographic entanglement entropy for the most general higher derivative gravity, *J. High Energy Phys.* 1508 (2015) 031, arXiv:1411.5579 [hep-th].

- [47] Y. Sun, H. Xu, L. Zhao, Thermodynamics and holographic entanglement entropy for spherical black holes in 5D Gauss–Bonnet gravity, arXiv:1606.06531 [hep-th].
- [48] X.O. Camanho, J.D. Edelstein, Causality in AdS/CFT and Lovelock theory, arXiv:0912.1944 [hep-th].
- [49] R.G. Cai, Gauss–Bonnet black holes in AdS spaces, Phys. Rev. D 65 (2002) 084014, arXiv:hep-th/0109133.
- [50] C.V. Johnson, Gauss–Bonnet black holes and holographic heat engines beyond large N, arXiv:1511.08782 [hep-th].
- [51] M. Cvetič, S. Nojiri, S.D. Odintsov, Black hole thermodynamics and negative entropy in de Sitter and Anti-de Sitter Einstein–Gauss–Bonnet gravity, Nucl. Phys. B 628 (2002) 295.
- [52] X.O. Camanho, J.D. Edelstein, Causality constraints in AdS/CFT from conformal collider physics and Gauss–Bonnet gravity, arXiv:0911.3160 [hep-th].
- [53] R.G. Cai, L.M. Cao, L. Li, R.Q. Yang, P–V criticality in the extended phase space of Gauss–Bonnet black holes in AdS space, J. High Energy Phys. 09 (2013) 005, arXiv:1306.6233 [gr-qc].
- [54] R. Banerjee, D. Roychowdhury, Critical phenomena in Born–Infeld AdS black holes, Phys. Rev. D 85 (2012) 044040, <http://dx.doi.org/10.1103/PhysRevD.85.044040>, arXiv:1111.0147 [gr-qc].
- [55] J.M. Maldacena, Wilson loops in large N field theories, Phys. Rev. Lett. 80 (1998) 4859, arXiv:hep-th/9803002.
- [56] V. Balasubramanian, S.F. Ross, Holographic particle detection, Phys. Rev. D 61 (2000) 044007, arXiv:hep-th/9906226.